Development of Nanofiller-Modulated Polymeric Oxygen Enrichment Membranes for Reduction of Nitrogen Oxides in Coal Combustion

Dr. Jianzhong Lou
North Carolina A&T State University
DE-FG26-06NT42742

Commercial Membrane Cartridges

- Hollow-fiber

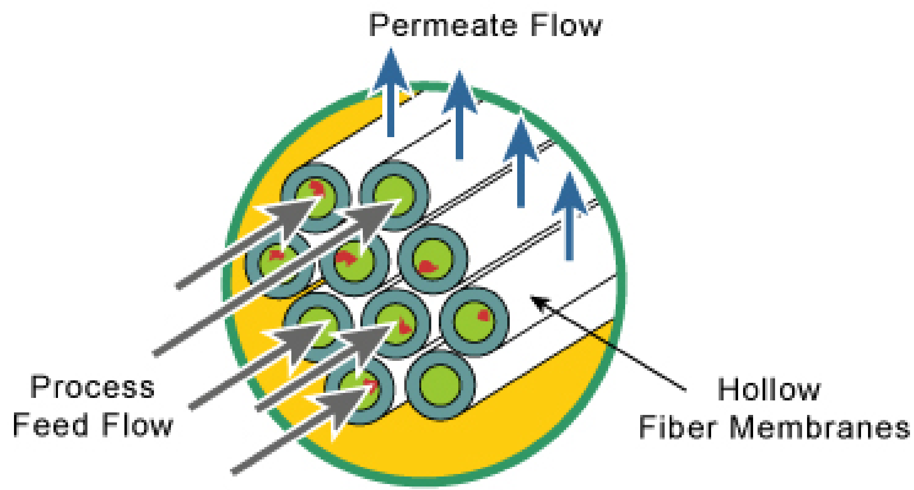

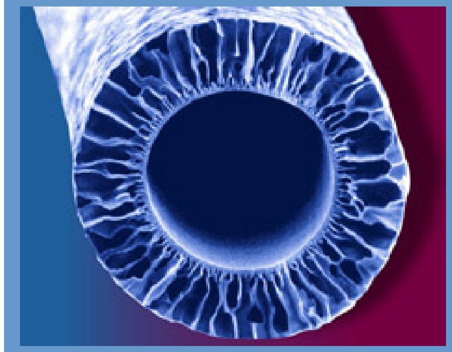

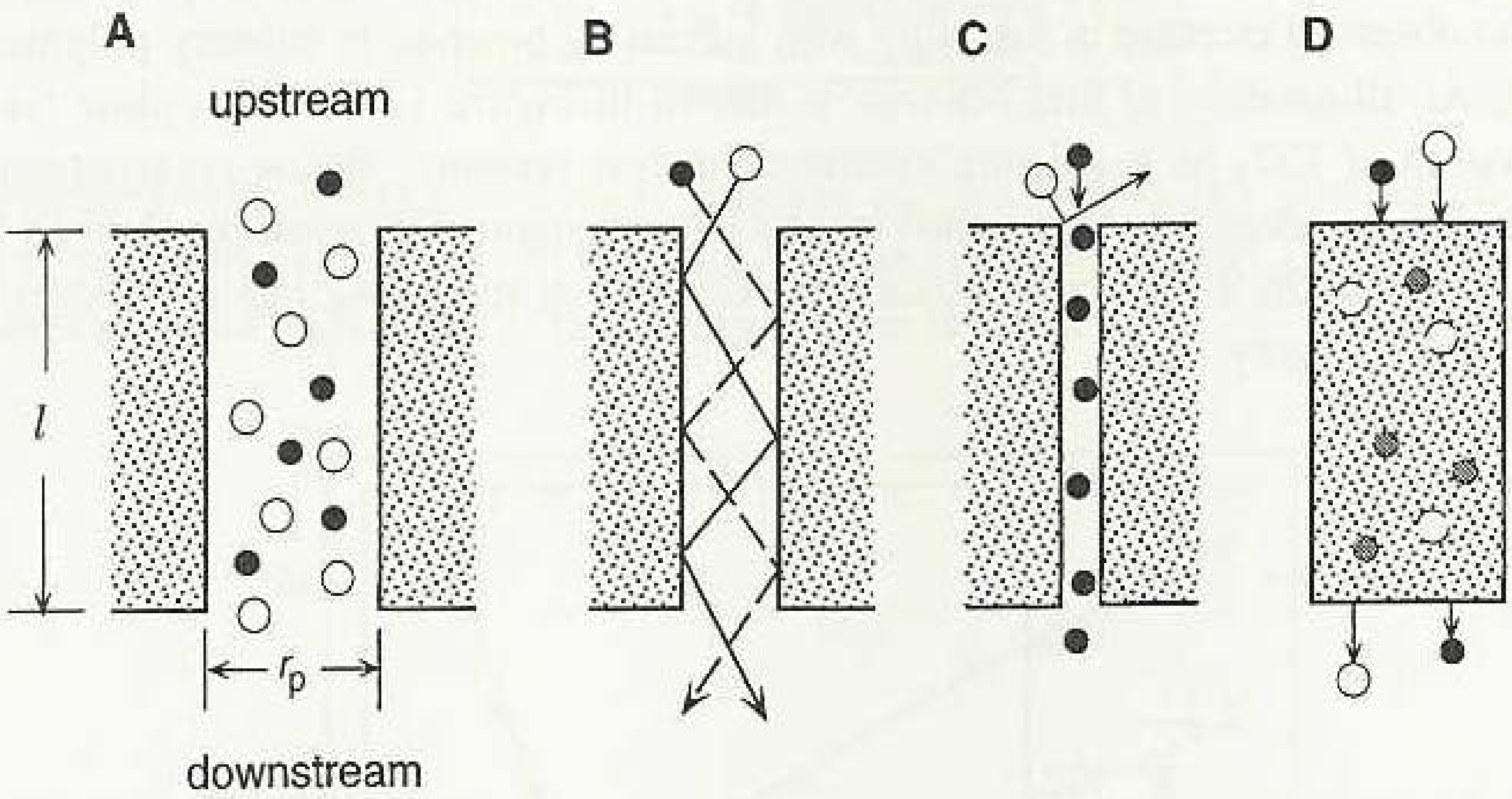

Figure 12-7 Illustration of the membrane transport of two differently sized molecules by various mechanisms. From left to right: **A** *viscous flow* through large pores of radii, r_p (no separation); **B** *Knudsen flow* (separation based upon difference in molecular weights); **C** *molecular sieving* (separation due to relative diffusive rates and surface sorption on pore walls); and **D** *solution-diffusion* through a dense membrane (separation based upon relative solubility and diffusivity).

PDMS Carbon Nanotube Membrane

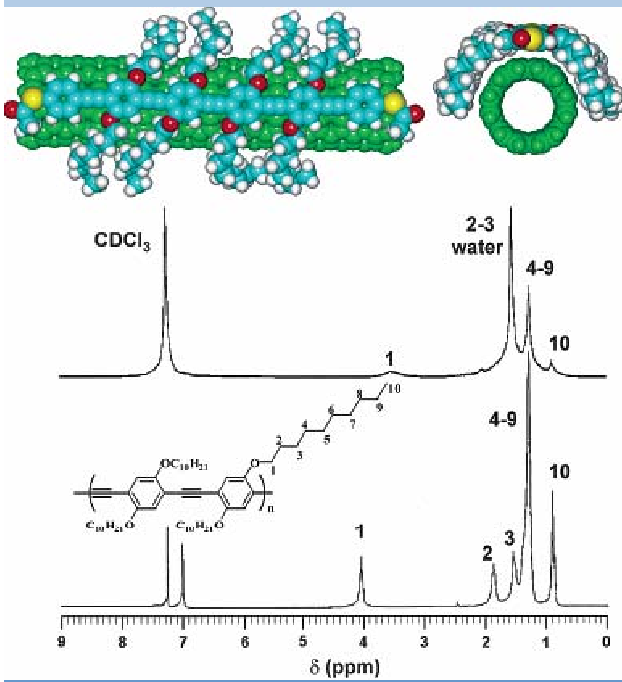

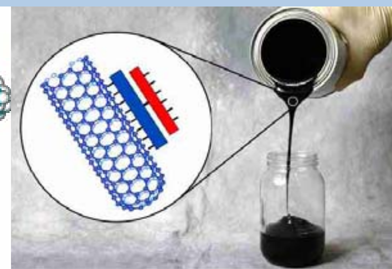

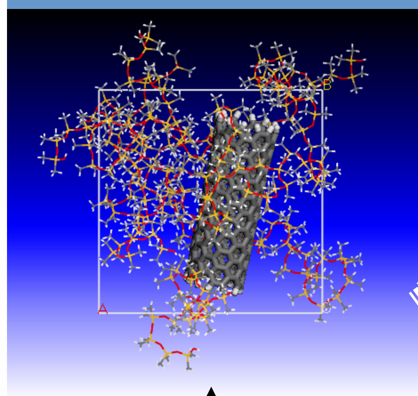

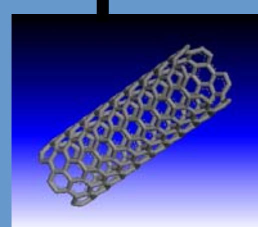

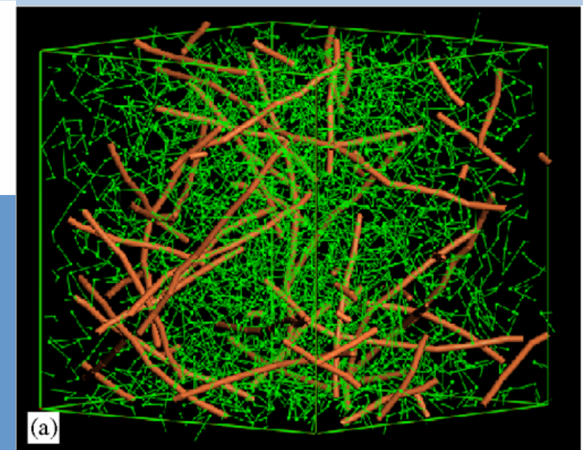

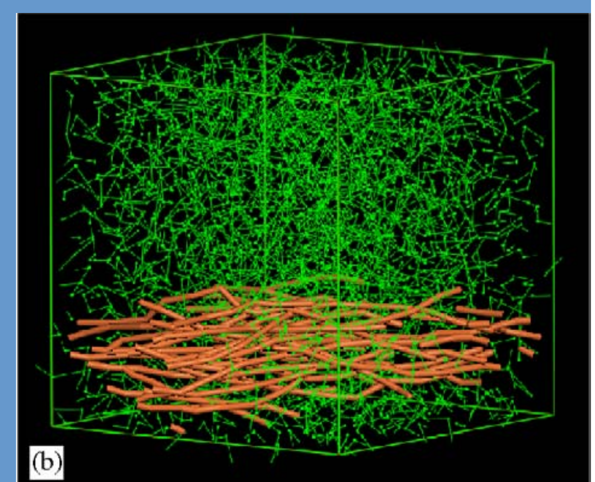

A molecular model of **1a***n*)1.5-SWNT(6,6) complex (top) and 1H NMR spectra (300 MHz, CDCl3) of **1a** (bottom) and **a**-SWNTsHiPco complex (middle). [Jian Chen etc. *J.Am. Chem. Soc.* **2002**, *124*, 9034-9035]

Molecular Modeling and Simulations

Nanofiller

Nanocomposite

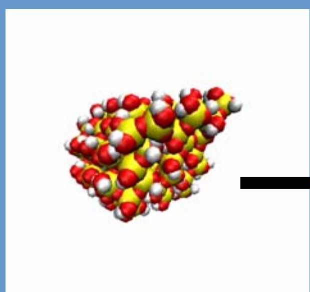

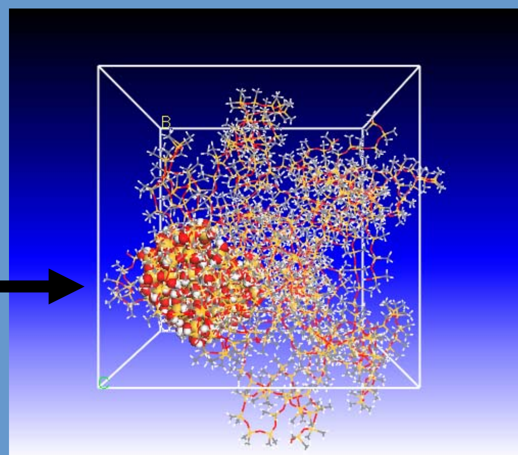

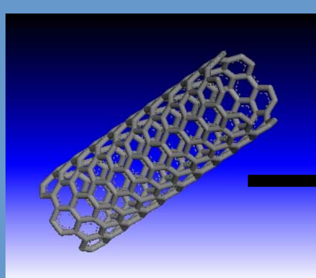

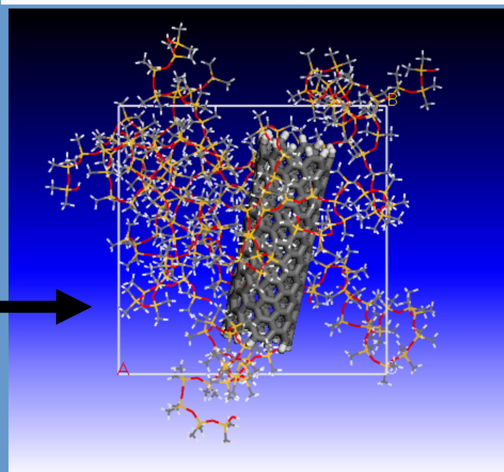

Modified GROMOS force field

$$E_{PE} = \sum_{bonds} k_r \left(r - r_0\right)^2 + \sum_{angles} k_\theta \left(\theta - \theta_0\right)^2 + \sum_{impropers} k_\xi \left(\xi - \xi_0\right)^2$$

$$+ \sum_{torsional} k_\Phi \left[1 + \cos\left(n\theta - \delta\right)\right] + \sum_i \sum_{j>i} f_{ij} \left\{ \frac{q_i q_j e^2}{r_{ij}} + 4\varepsilon_{ij} \left[\left(\frac{\sigma_{ij}}{r_{ij}}\right)^{12} - \left(\frac{\sigma_{ij}}{r_{ij}}\right)^6 \right] \right\}$$

Bonds	k_b (10^5/kJ mol^{-1} nm^{-2})			b_0 (nm)
Si–O	2.5080			0.160
Si–CH_3	2.5080			0.188
Angles	k_Θ (kJ/mol^{-1} rad^{-2})			Θ_0 (deg)
Si–O–Si	118.4			114.0
O–Si–O	791.2			109.5
O–Si–CH_3	418.4			109.5
CH_3–Si–CH_3	418.4			109.5
Dihedrals	k_φ (kJ mol^{-1})		n	δ
CH_3–Si–O–Si	3.77		3	0
Si–O–Si–CH_3	3.77		3	0
Si–O–Si–O	3.77		3	0
O–Si–O–Si	3.77		3	0
Nonbonded	ϵ (kJ mol^{-1})	σ (nm)	$q(e)$	(a.m.u)
Si	2.4480	0.3385	0.3	28.080
O	0.8493	0.2955	−0.3	15.999
CH_3 (PDMS)	0.7532	0.3786	0	15.035
He	0.0850	0.2580	0	4.003
H_2	0.3076	0.2950	0	2.016
Ar	0.9977	0.3400	0	39.948
N_2	0.7898	0.3700	0	28.013
O_2	0.9145	0.3500	0	31.998
CH_4	1.2466	0.3733	0	16.043

Gas-Separation Membrane Definitions

Mass transfer flux $J_A = P_A\left(\frac{dp_A}{dx}\right) = D_A\left(\frac{dc_A}{dx}\right)$

p_A partial pressure of gas molecule A

c_A concentration of gas molecule A

P_A Permeability of polymer for gas molecule A

D_A Difusion coefficient of gas molecule A inside polymer

$$S_A = \frac{c_A}{p_A}$$

S_A Solubility of gas molecule A inside polymer

Separation factor (also called selectivity) $\alpha_{A/B} = \frac{P_A}{P_B}$

Table 12-4 Applications for Polymeric Membranes in Gas Separations

Separations	Suitable Polymers
O_2/N_2	Silicone rubber Polysiloxane-*block*-polycarbonate Polysulfone Ethylcellulose Poly[(1-trimethylsilyl)-1-propyne] Polypyrrolone Polytriazole Polyaniline
H_2 from CO, CH_4, N_2	Polysulfone
Acid gases (CO_2 and H_2S) from hydrocarbons (e.g., natural gas and enhanced oil-recovery)	Cellulose acetate Poly(vinyl chloride) Polysulfone Polyetherimide
Hydrocarbon vapors from air	Silicone rubber

Table 12-7 Kinetic Diameters and Lennard-Jones Potential Well Depth* of Important Gases

Gas:	He	H_2	CO_2	O_2	N_2	CO	CH_4
Kinetic diameter (Å)	2.6	2.89	3.3	3.46	3.64	3.76	3.80
ε/k (K)	10.2	59.7	195	107	71.4	91.7	149
σ (Å)	2.55	2.83	3.94	3.47	3.80	3.69	3.76

*See text footnote for identification of the Lennard-Jones ε/k and σ parameters.

Table 12-5 Gas Permeability and Permselectivity of Representative Polymer (at 25° to 35°C)

Polymer	$P(O_2)$*	$\frac{P(O_2)}{P(N_2)}$	$P(CO_2)$	$\frac{P(CO_2)}{P(CH_4)}$
Rubbery Polymers				
High-density polyethylene ($\rho = 0.964$)	0.4	2.9	1.7	4.4
Butyl rubber	1.3	3.9	5.8	6.6
Low-density polyethylene ($\rho = 0.914$)	2.9	3.0	12.6	4.3
Natural rubber	24	3.0	134	4.7
Silicone rubber	610	2.2	4,553	3.4
Glassy Polymers				
Poly(ethylene terephthalate) ($X_c = 0.50$)	0.06	4.5	0.30	—
Cellulose acetate	0.68	3.4	5.5	28
Polysulfone	1.3	5.2	4.9	23
Polycarbonate	1.5	5.2	6.0	23
Polystyrene	2.6	3.3	10.5	—
Poly(2,6-dimethyl-1,4-phenylene oxide)	18	5.0	59	15
Poly(4-methylpentene-1)	29	4.4	93	—
Poly[1-(trimethylsilyl)-1-propyne]	7,200	1.7	19,000	4.4

* Permeability in barrers [10^{-10} cm^3 (STP)-cm/(cm^2-s-cm Hg)]

Permeability of Polydimethylsiloxane

Table 12-1 Permeability Coefficients of Selected Polymers at 25°C*

Polymer	$P(O_2)^{\dagger}$
Poly(vinyl alcohol)	~0.0001
Polyacrylonitrile	~0.002
Poly(vinylidene chloride)	0.012
Polymethacrylonitrile	0.012
Poly(ethylene terephthalate)	0.42
Poly(vinyl chloride)	0.48
Poly(vinyl acetate)	3.3
Polypropylene	10.8
Polyethylene (LDPE)	30.0
Polyisobutylene	90.0
Polydimethylsiloxane	~3000

*Data taken from ref. 1.

†$P \times 10^{11}$ cm^3-cm/cm^2-sec cmHg at 0% humidity

‡$P \times 10^{11}$ g-cm/cm^2 sec cmHg

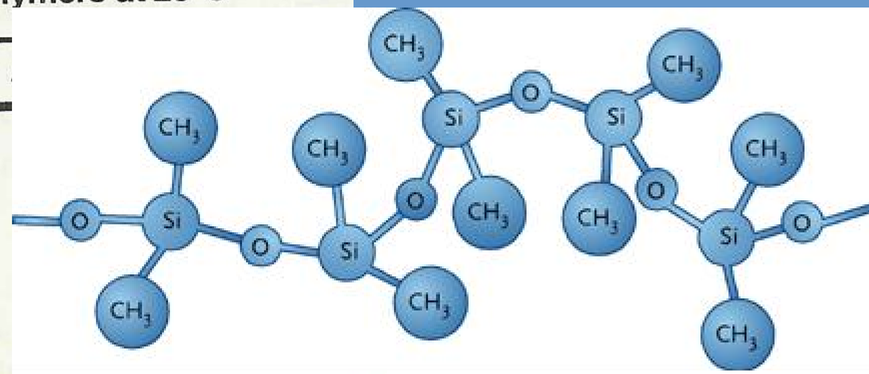

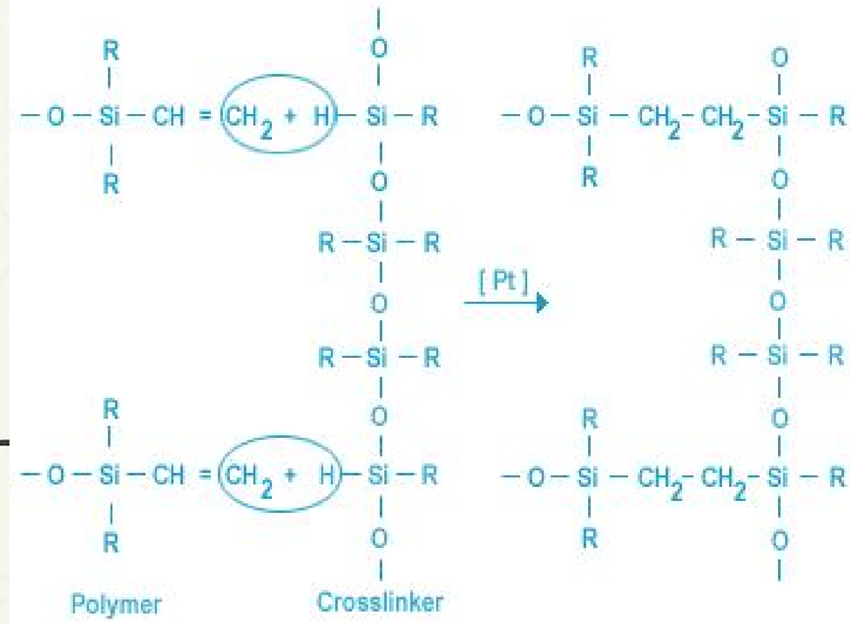

Measurement of Diffusion Coefficient

$$\boxed{D = \frac{\ell^2}{6\theta}} \quad (12.22)$$

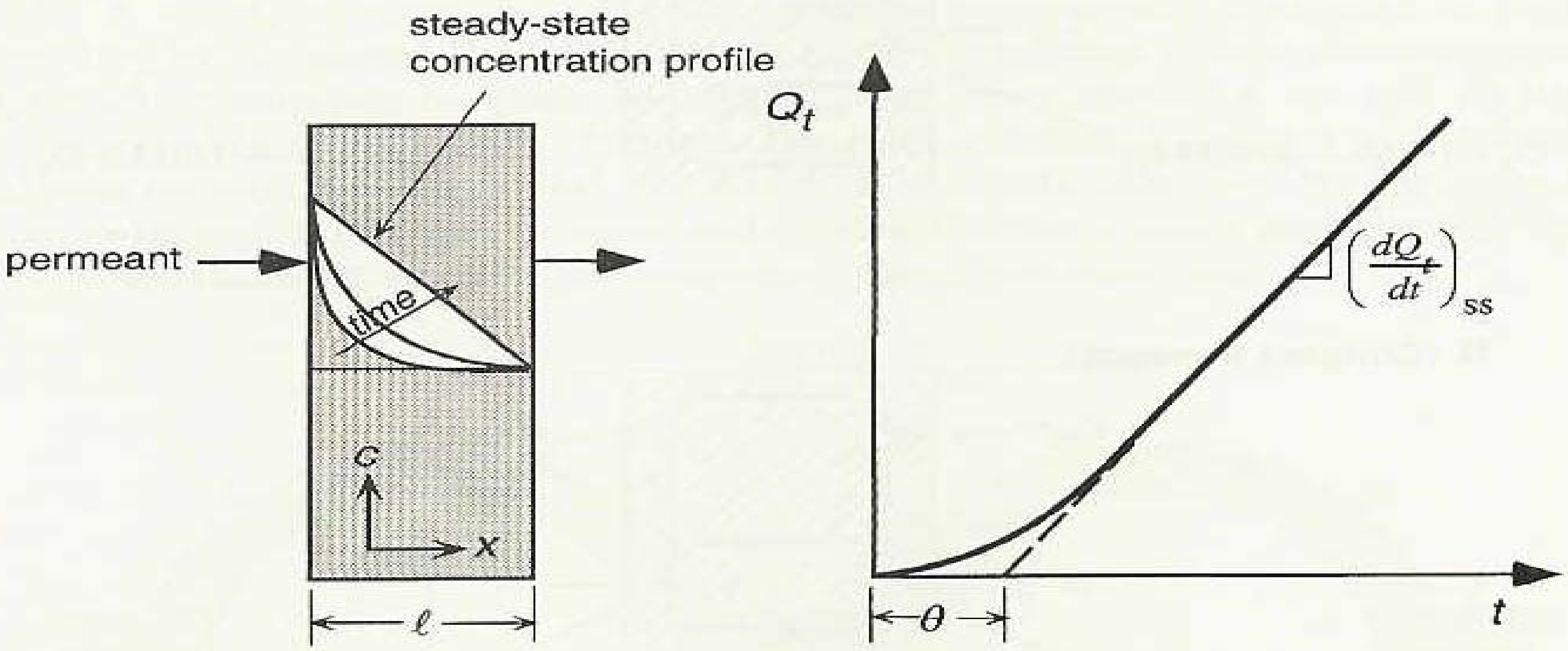

Figure 12-10 Plot of the amount of permeant versus time for a flat film illustrated at the left. The slope of the linear portion of the curve gives the steady-state permeability, while the intercept with the time axis yields the time lag, θ, from which the apparent diffusion coefficient can be obtained (eq. 12.22). The increase in permeant concentration in the film up to the attainment of steady state is illustrated at the left.

Measurement of Solubility

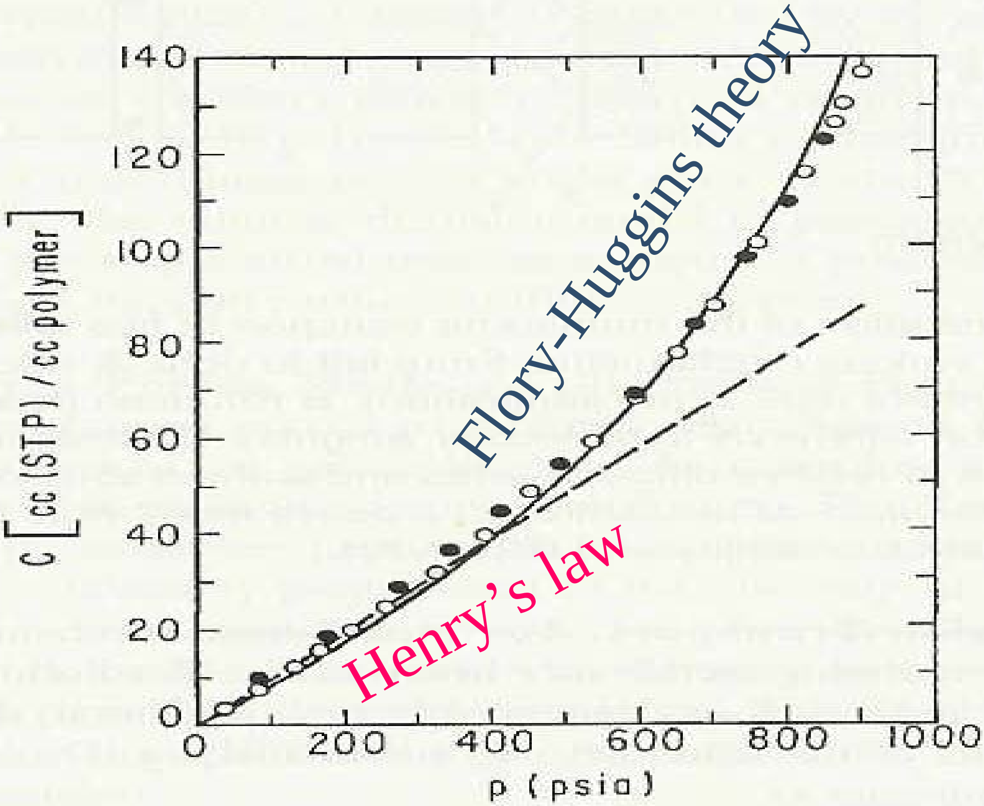

Figure 12-8 Sorption isotherm of CO_2 in silicone rubber at 35°C. Data points give CO_2 concentrations measured at different pressures during sorption (○) and desorption (●). The solid line represents the fit by the Flory–Huggins equation; the broken line represents Henry's law behavior. (Reprinted with permission from G. K. Fleming and W. J. Koros, *Macromolecules*, **19**, 2285 (1986). Copyright 1986 American Chemical Society.)

Experimental set up

- Preferred method for application of thin, uniform films to flat substrates.
- The polymer solution placed on the substrate is rotated at high speed in order to spread the fluid by centrifugal force.
- Rotation is continued for some time, with fluid being spun off the edges of the substrate, until the desired film thickness is achieved.

Figure 1: SEM picture of neat polymer and filled polymer on metallic substrate

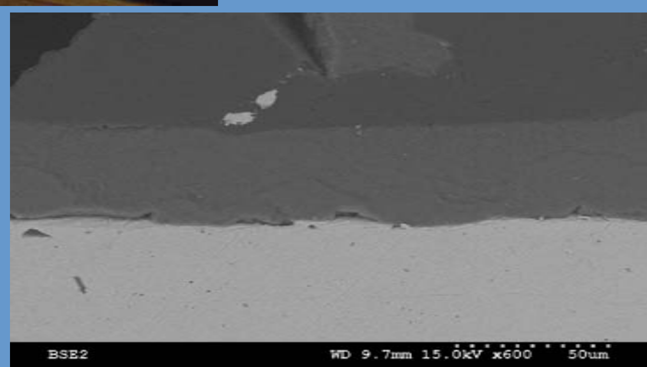

Neat polymer 18 μm thick

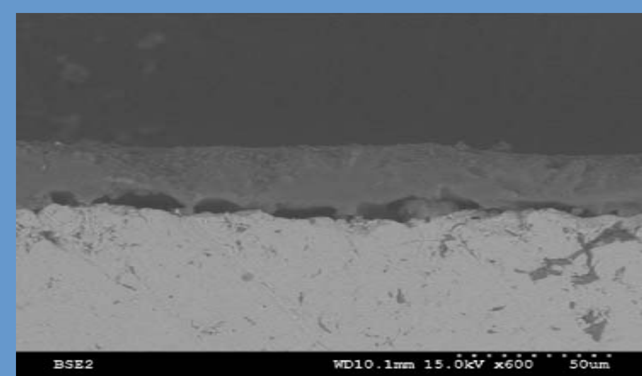

Filled polymer 28 μm thick

PDMS Carbon Nanotube Membrane

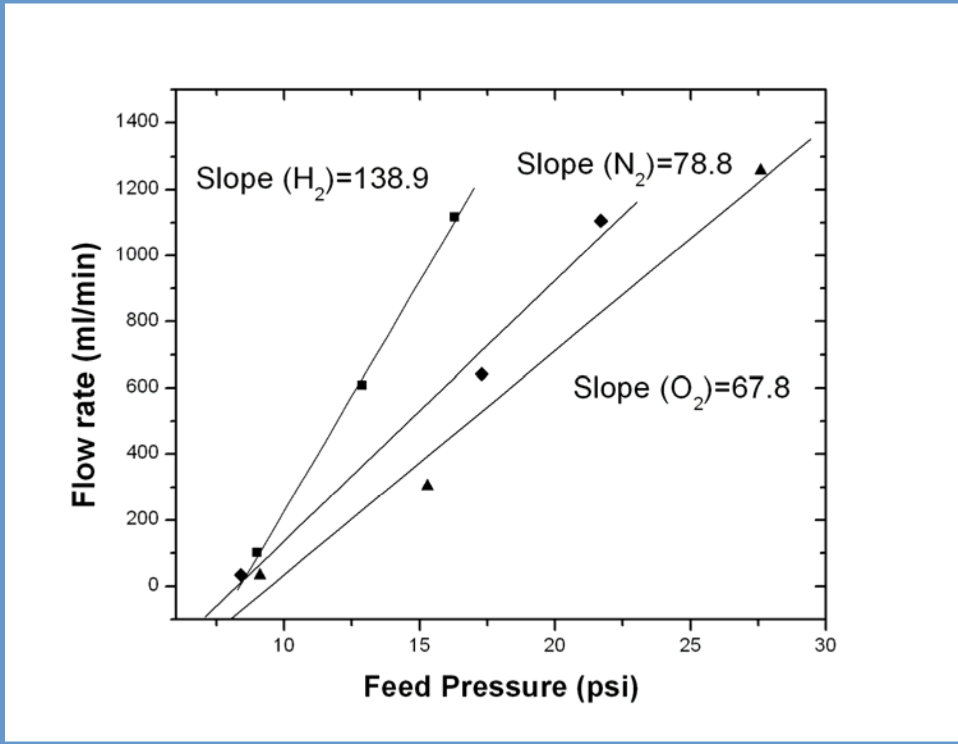

Selectivity	Neat PDMS	PDMS+MWNT
Oxygen/Nitrogen	1.97	0.86
Hydrogen/Oxygen	1.01	2.05

PDMS-Silica Membrane

Neat PDMS

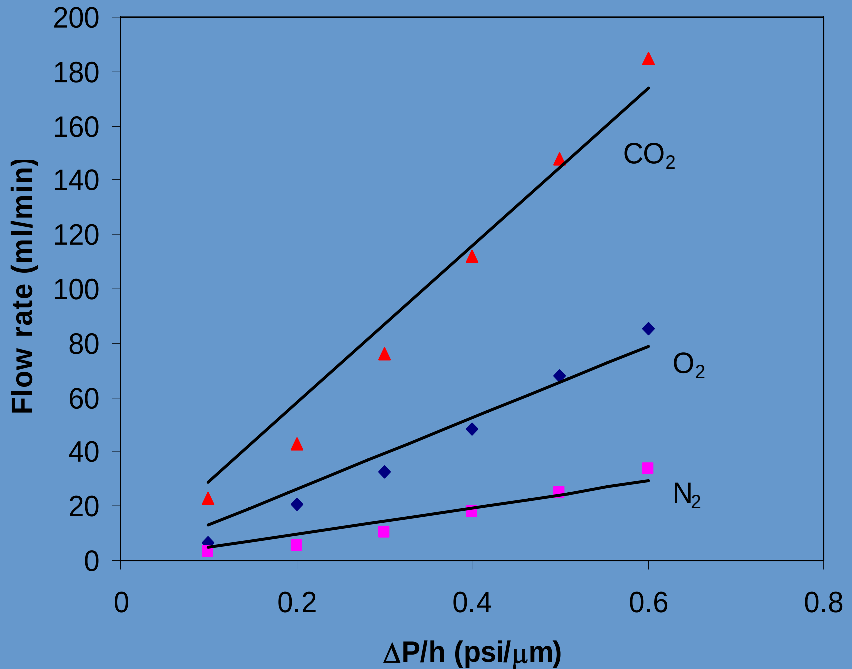

Filled PDMS

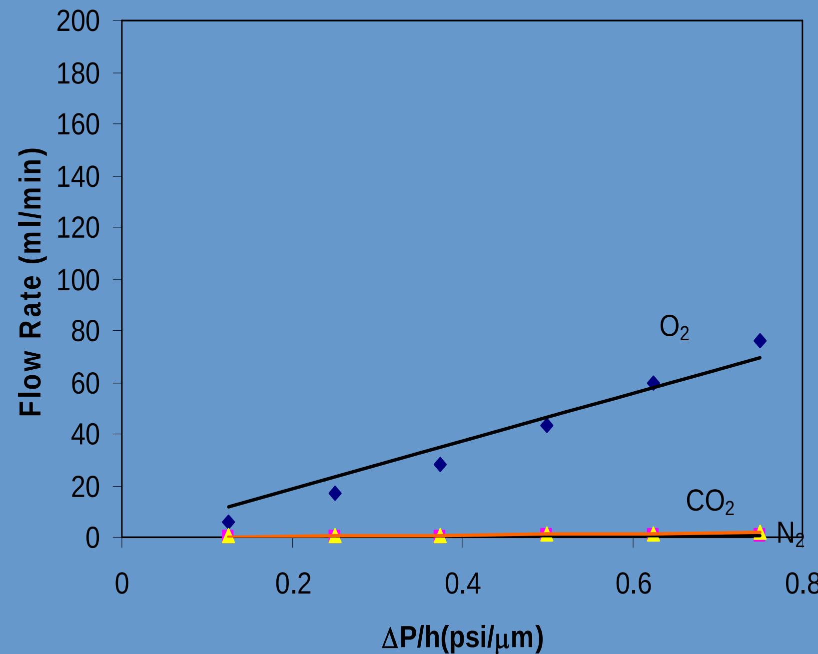

$$J_A = P_A\left(\frac{dp_A}{dx}\right) = D_A\left(\frac{dc_A}{dx}\right)$$

$$\alpha_{Oxygen\,/\,Nitrogen} = \frac{P_{O2}}{P_{N2}} = \frac{J_{O2}\cdot p_{N2}}{J_{N2}\cdot p_{O2}}$$

Difficulty in Measuring Diffusion Coefficient

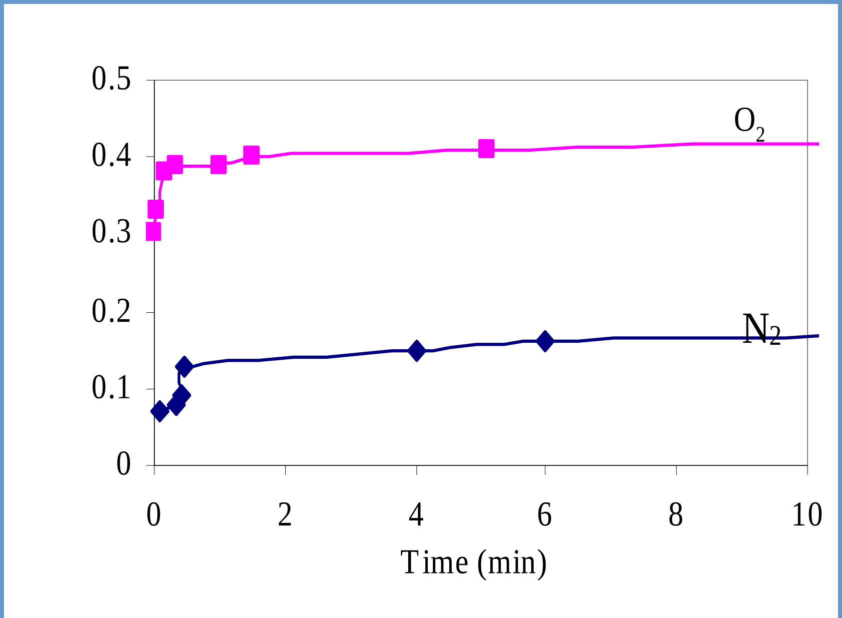

Response of permeate pressure for neat PDMS- time lag method

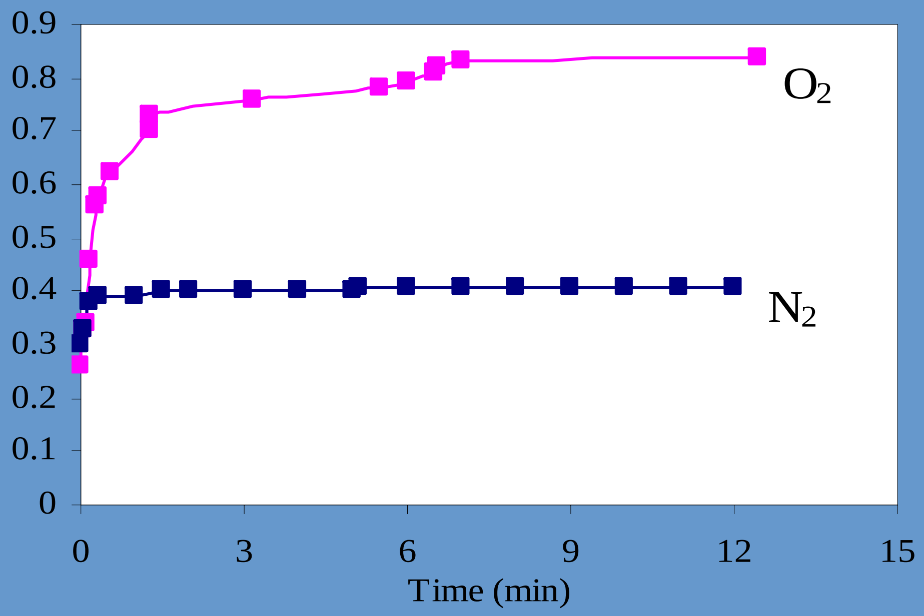

Response of permeate pressure for filled PDMS- time lag method

Selectivity of O_2/N_2	PDMS	Filled PDMS
$\alpha_{A/B}$	2.04	8.54

Conclusion

- Nanofillers have significant impact on both permeability and permselectivity of polymers.
- Whether or not the selectivity was controlled by the size of the molecules and the interactions between the molecules and the surfaces of the fillers remain to be investigated.
- Since silicone polymers are well known for their high free volume characteristics, this trade-off of slight reduction in permeability and drastic increase in selectivity seems to be commercially attractive.
- Molecular dynamics simulation model has been established to further the study of diffusion and solution of oxygen molecules in a nanofiller (nanotube and nanosilica) filled polymer system. This will lead to better understanding of filled polymer and guide the further experimental development of novel membrane in the next project period.

References

- [1] T. C. Merkel; Freeman, B. D.; Spontak, R. J.; He, Z.; Pinnau, I.; Meakin, P.; Hill, A. J., "Sorption, transport, and structural evidence for enhanced free volume in poly(4-methyl-2-pentyne)/fumed silica nanocomposite membranes", Chemistry of Materials, 15(1), 109-123 (2003).

- [2] N. F. A. van der Vegt, W. J. Briels, M. Wessling, and H. Strathmann, "Free energy calculations of small molecules in dense amorphous polymers. Effect of the initial guess configuration in molecular dynamics studies," J. Chem. Phys. 1996 (105). pp. 8849-8857

- [3] Jian Chen etc. *J.Am. Chem. Soc.* **2002**, *124*, 9034-9035

Acknowledgements:

Financial support from DOE DE-FG26-06NT42742

Thank you for your attention.